

Quench dynamics and bulk-edge correspondence in nonlinear mechanical systems

Motohiko Ezawa

Department of Applied Physics, University of Tokyo, Hongo 7-3-1, 113-8656, Japan

We study a topological physics in a one-dimensional nonlinear system by taking an instance of a mechanical rotator model with alternating spring constants. This nonlinear model is smoothly connected to an acoustic model described by the Su-Schrieffer-Heeger model in the linear limit. We numerically show that quench dynamics of the kinetic and potential energies for the nonlinear model is well understood in terms of the topological and trivial phases defined in the associated linearized model. It indicates phenomenologically the emergence of the edge state in the topological phase even for the nonlinear system, which may be the bulk-edge correspondence in nonlinear system.

I. INTRODUCTION

Topological insulators^{1,2} were originally discovered in inorganic solid state materials. However, it is now well recognized that topological physics is ubiquitous in various systems such as acoustic^{3–12}, mechanical^{13–29}, photonic^{30–37} and electric circuit^{38–53} systems. They are called artificial topological systems. The merit of them is that it is possible to fabricate ideal systems comparing to natural solid state materials. Another merit of artificial topological systems is that nonlinearity is naturally introduced into them.

Topological physics is mostly studied in linear systems. There are only a few studies on it in nonlinear systems^{53–56} because the study of the topological properties is not straightforward. One of the reasons is that it is a formidable problem to obtain a band structure and a topological number in a generic nonlinear system. Recently, it is proposed to account for the topological properties in nonlinear systems phenomenologically based on the bulk-edge correspondence well established in the linear theory⁵⁶. It seems to work provided that the nonlinear theory is continuously connected to a linear theory where the topological number is well defined. One may say that the topological properties are inherited from a linear theory to a nonlinear theory. It is an interesting problem to explore other systems which share similar properties.

A good signal to detect the topological phase transition is to study quench dynamics starting from one of the edges in the case of one dimension based on the bulk-edge correspondence⁵⁷. There is almost no time evolution and the state remains almost localized at the edge for a topological phase. It is because the initial state is almost given by the topological localized edge state, which has no dynamics. On the other hand, the state rapidly spreads into the bulk for a trivial phase because the initial state is composed of bulk eigen functions. Although the usefulness of quench dynamics has been established in a linear system, it is also useful in a nonlinear system⁵⁶.

In this paper, we investigate a one-dimensional mechanical rotator model with alternating spring constants: See Fig.1. It is a nonlinear generalization of the Su-Schrieffer-Heeger (SSH) model. We solve the quench dynamics of a mechanical rotator model as an initial condition problem, where only one rotator at the left-most edge is excited initially. The potential and kinetic energies exhibit distinct behaviors depending on whether the system is in the topological or trivial phase

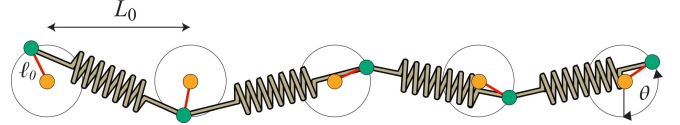


FIG. 1: Illustration of the mechanical rotator model. Two adjacent rotators are connected by a spring with the spring constant κ_j . A rotator colored in green rotates around a center colored in orange with the radius ℓ_0 . All centers are on a line, and the distance between two adjacent centers is L_0 .

defined in the linearized model. Namely, after enough time, they are well localized in the topological phase, while they are spread over the bulk in the trivial phase. These phenomena are understood in terms of the emergence of the topological edge state in the topological phase. It would represent the bulk-edge correspondence in nonlinear system.

II. MECHANICAL ROTATOR MODEL

We consider a mechanical rotator model¹³ as illustrated in Fig.1. We place rotators indexed by the number j , $j = 1, 2, \dots, N$. Each rotator has the radius ℓ_0 , and its center is fixed at the position $(jL_0, 0)$ on the x axis, with L_0 the distance between two adjacent centers. The dynamical variables are angles θ_j for rotators j .

The Hamiltonian of the system consists of the kinetic energy U^K , the potential energy of the springs U^{spring} and the gravitational energy of the U^g ,

$$H = U^K + U^{\text{spring}} + U^g. \quad (1)$$

They are given by

$$U^K = \sum_j U_j^K, \quad U_j^K = \frac{m}{2} \dot{\theta}_j^2 \quad (2)$$

with the mass m ,

$$U^g = -g \sum_j \cos \theta_j \quad (3)$$

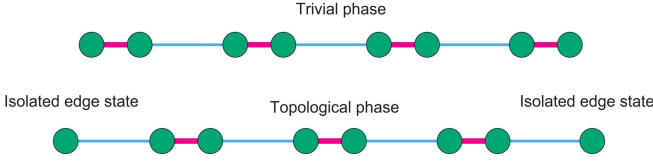


FIG. 2: Illustration of the trivial and topological phases in the SSH model. There are two isolated edge states in the topological phase, while all of the sites are dimerized in the trivial phase. Magenta and cyan lines represent strong and weak bondings κ_j in Eq.(10), respectively. This illustration is argued to hold even in nonlinear system described by Eq.(9).

with the gravitational constant g , and

$$U^{\text{spring}} = \sum_j U_j^{\text{spring}}, \quad (4)$$

$$U_j^{\text{spring}} = \frac{1}{2} \kappa_j (L_j(\theta_j, \theta_{j+1}) - L)^2, \quad (5)$$

where $L_j(\theta_j, \theta_{j+1})$ is the length of the spring between j and $j+1$ nodes,

$$L_j(\theta_j, \theta_{j+1}) = \sqrt{[L_j^x(\theta_j, \theta_{j+1})]^2 + [L_j^y(\theta_j, \theta_{j+1})]^2} \quad (6)$$

with

$$L_j^x(\theta_j, \theta_{j+1}) = \ell_0 \sin \theta_{j+1} - \ell_0 \sin \theta_j + L_0, \quad (7)$$

$$L_j^y(\theta_j, \theta_{j+1}) = \ell_0 \cos \theta_{j+1} - \ell_0 \cos \theta_j. \quad (8)$$

The equation of motion is given by

$$m\ddot{\theta}_j = -g \sin \theta_j - \frac{\partial U^{\text{spring}}}{\partial \theta_j}. \quad (9)$$

The spring constant is assumed to be alternating,

$$\kappa_j = \kappa \left(1 + \lambda (-1)^j \right), \quad (10)$$

where the dimerization is controlled by λ with $|\lambda| \leq 1$. For $\lambda < 0$, the spring constant κ_j with odd (even) j is strong (weak). On the other hand, for $\lambda > 0$, the spring constant κ_j with odd (even) j is weak (strong): See Fig.2.

III. LINEARIZED MODEL

Provided the angle θ_j is small enough, the potential energy is well approximated by the harmonic potential,

$$U^{\text{spring}} = \frac{\ell_0^2}{2} \sum_j \kappa_j (\theta_{j+1} - \theta_j)^2, \quad (11)$$

and the equation of motion is obtained as

$$m\ddot{\theta}_j = -g\theta_j - \ell_0^2 \sum_j \kappa_j (\theta_j - \theta_{j+1}) + \kappa_{j-1} (\theta_j - \theta_{j-1}), \quad (12)$$

which is a linearized model.

Eq.(12) is rewritten in the form of

$$m\ddot{\theta}_j = \sum_j K_{ij} \theta_j, \quad (13)$$

where

$$K_{ij} = -\delta_{ij} (g + \ell_0^2) + \ell_0^2 (\kappa_j \delta_{i,j+1} + \kappa_{j-1} \delta_{i,j-1}) \quad (14)$$

is identical to the SSH Hamiltonian. After a Fourier transformation, we have

$$K(k) = -(g + \ell_0^2) I_2 + \kappa \begin{pmatrix} 0 & 1 - \lambda e^{-ik} \\ 1 - \lambda e^{ik} & 0 \end{pmatrix}. \quad (15)$$

It is known^{13,14} that the system is topological for $\lambda < 0$ and trivial for $\lambda > 0$. There are two isolated edge states in the limit $\lambda \simeq -1$, while all of the states are dimerized in the limit $\lambda \simeq 1$: See Fig.2.

The topological number associated with the SSH Hamiltonian is the chiral index defined by

$$\Gamma = \int_0^{2\pi} \text{Tr} [\sigma_z K^{-1} \partial_k K] dk, \quad (16)$$

where K is given by Eq.(15). We obtain $\Gamma = 1$ for $\lambda < 0$ and $\Gamma = 0$ for $\lambda > 0$.

Our interest is the effect of the nonlinearity based on Eq.(9) instead of the linear equation of motion (12).

IV. NONLINEAR QUENCH DYNAMICS AND BULK-EDGE CORRESPONDENCE

The quench dynamics starting from a state localized at one edge well captures the topological phase transition in linear systems⁵⁷, where the eigenfunctions are easily obtained and a topological number is well defined. In the topological phase, there are topological edge states well localized at edges, which is known as the bulk-edge correspondence. If we excite only one edge site, the most component is dominated by a topological edge state. The topological edge state remains as it is after time evolution. On the other hand, there is no such localized edge state in the trivial phase. Hence, all of the components of the initial state are bulk eigenfunctions. They are spread into the bulk after the time evolution. Thus, it is possible to distinguish topological and trivial phases by checking whether the state is localized or spread into the bulk.

The above observation is also applicable even for nonlinear systems⁵⁶. The existence of the localized topological edge state is obscure in nonlinear systems because it is not possible to diagonalize the Hamiltonian and obtain eigenfunctions. Nevertheless, the quench dynamics shows distinct behaviors between the topological and trivial phases as in the case of the linear system. Thus, the quench dynamics starting from one of the edges is a strong signal to detect a topological phase transition.

We numerically solve the equation of motion (9) with the initial condition $\theta_j(t=0) = \theta_0 \delta_{j,1}$ and $\dot{\theta}_j(t=0) = 0$. If

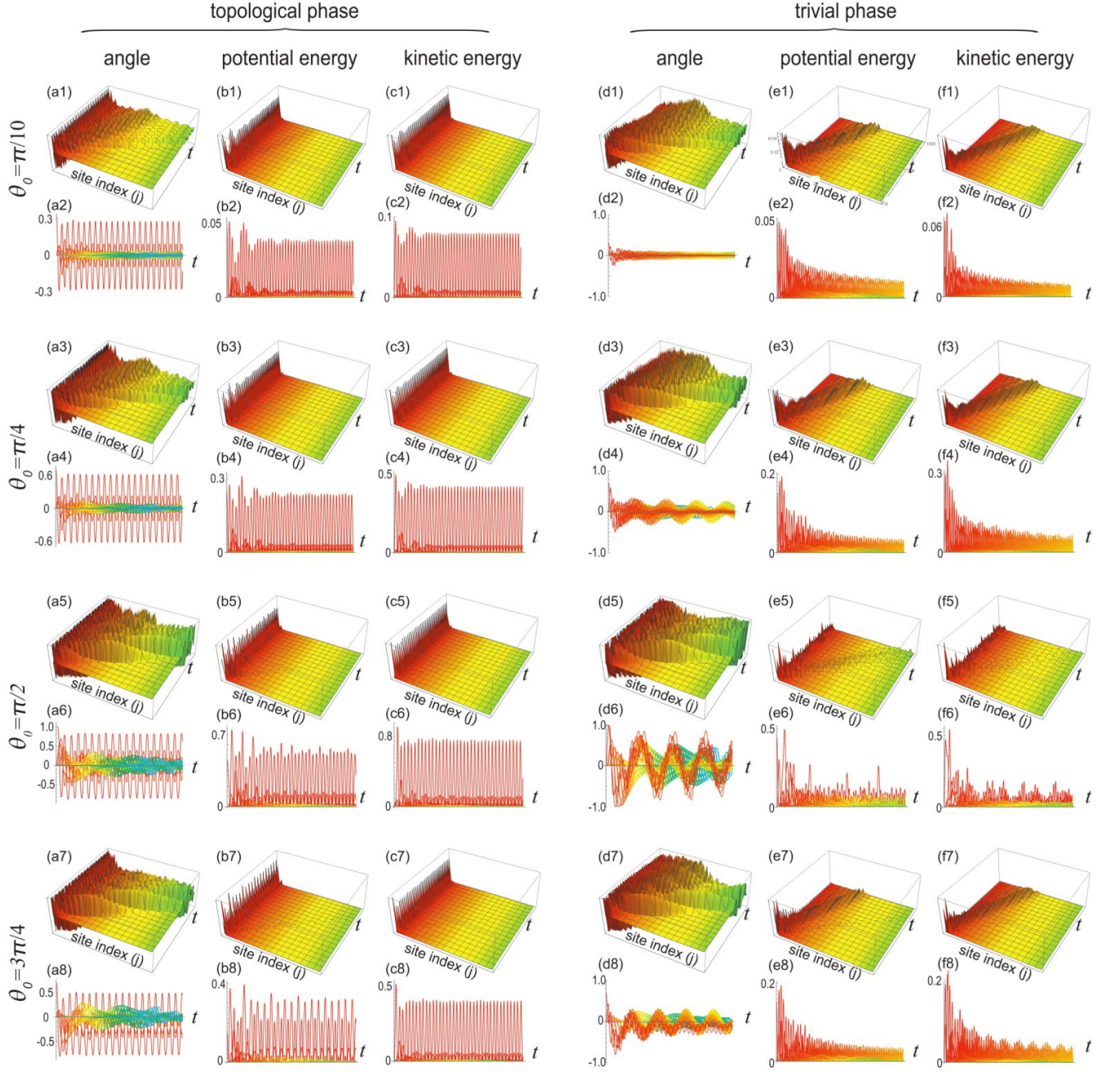


FIG. 3: Time evolution of the angle $\sin \theta_j$ for (a1)~(a8) and (d1)~(d8), the potential energy U_j^{spring} for (b1)~(b8) and (e1)~(e8), and the kinetic energy U_j^K for (c1)~(c8) and (f1)~(f8). (a1)~(c8) topological phase with $\lambda = -0.5$, and (d1)~(f8) trivial phase with $\lambda = 0.5$. (a1)~(f2) $\theta_0 = \pi/10$, (a3)~(f4) $\theta_0 = \pi/4$, (a5)~(f6) $\theta_0 = \pi/2$, and (a7)~(f8) $\theta_0 = 3\pi/4$. (a1)~(f1), (a3)~(f3), (a5)~(f5) and (a7)~(f7) Bird's eye's view, and (a2)~(f2), (a4)~(f4), (a6)~(f6) and (a8)~(f8) Color plot of the time evolution. We have used a chain containing 100 sites. We have set $m = 0.01$, $g = 0.1$, $L_0 = 10$ and $\ell_0 = 1$. Color indicates the site index j , which is manifest in bird's eye's views.

$|\theta_0| \ll 1$, the system is well described by the linear equation (12). Otherwise, the system is nonlinear. We study a case $\theta_0 = \pi/10, \pi/4, \pi/2$ and $3\pi/4$ as typical examples.

We show the time evolution of $\sin \theta_j$, the potential energy U_j^{spring} and the kinetic energy U_j^K in Fig.3. The quench dynamics of $\sin \theta_j$ is significantly different between the topological and trivial phases. The amplitude of $\sin \theta_1$ at the left

edge site remains finite in the topological phase. On the other hand, the amplitude of $\sin \theta_1$ decreases in the trivial phase. The potential energy U_j^{spring} remains well localized at the left edge in the topological phase although the absolute value of $\sin \theta_j$ spreads into the bulk as shown in Fig.3(b). On the other hand, it moves as if it were a soliton in the trivial phase as shown in Fig.3(e). If $\theta_0 = \pi/2$, there remains a finite com-

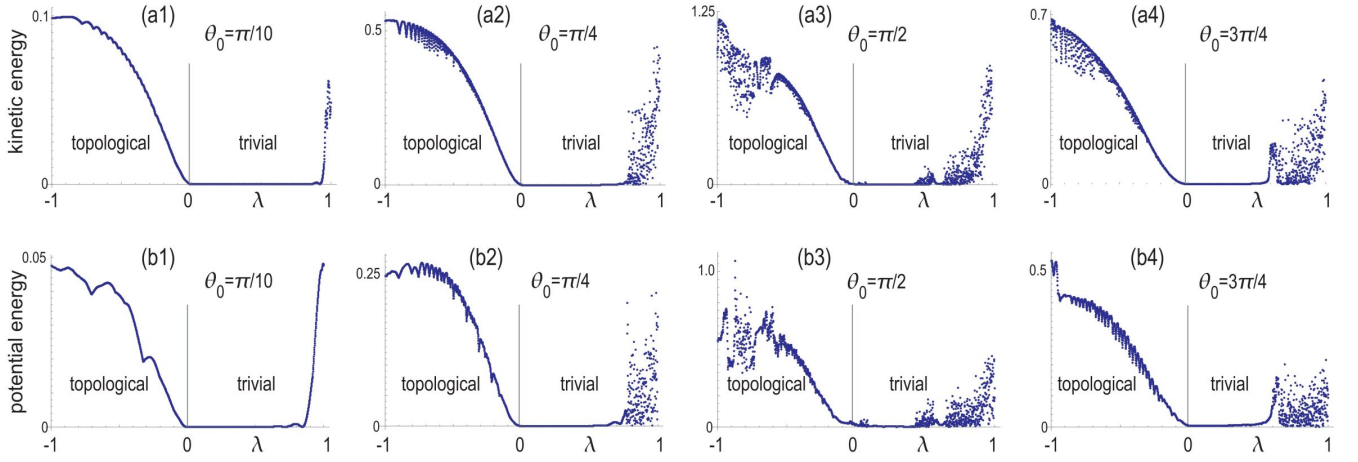


FIG. 4: (a1)~(a4) Kinetic energy at the edge U_1^K , and (b1)~(b4) the potential energy at the edge U_1^{spring} as a function of the initial position θ_0 after enough time. (a1) and (b1) $\theta_0 = \pi/10$, (a2) and (b2) $\theta_0 = \pi/4$, (a3) and (b3) $\theta_0 = \pi/2$, (a4) and (b4) $\theta_0 = 3\pi/4$. See the caption of Fig.3 for the parameters.

ponent in U_j^{spring} as well as a soliton-like propagation. This will be because that $\sin \theta_j$ takes a maximum for $\theta_0 = \pi/2$, where the dynamics is most enhanced and it takes longer time to reach a steady state.

We also show the time evolution of the kinetic energy U_j^K in Fig.3(c) and (f). The behavior of U_j^K is quite similar to that of U_j^{spring} .

The dynamics between $\theta_0 = \pi/4$ and $3\pi/4$ are very similar as shown in Fig.3. It will be due to the fact that $\sin \pi/4 = \sin 3\pi/4$ although we have $\cos \pi/4 \neq \cos 3\pi/4$. These results indicate a symmetry between the angle θ_1 and θ_2 satisfying the condition $\sin \theta_1 = \sin \theta_2$, where the dynamics is similar.

The potential and kinetic energies after enough time present a good signal for the topological phase transition comparing to the dynamics of $\sin \theta_j$. We show the kinetic energy U_j^K and the potential energy U_j^{spring} after enough time as a function of λ in Fig.4. It is finite for the topological phase with $\lambda < 0$, while it is almost zero for the trivial phase with $\lambda > 0$. These features are common for all initial conditions $\theta_0 = \pi/10, \pi/4, \pi/2$ and $3\pi/4$. It indicates the bulk-edge correspondence in nonlinear systems. It suggests the validity of the topological number (16) even in strong nonlinear regime.

A comment is in order with respect to finite components around $\lambda \simeq 1$ in Fig.4. They are interpreted as follows. In the limit $\lambda \simeq 1$, the system is almost dimerized as shown in Fig.2,

where there are no isolated sites at the both edges. In this limit, the energy is not well transferred to the bulk because the energy is localized in the dimer located at the edge to which the energy is injected, resulting in finite components around $\lambda \simeq 1$.

V. DISCUSSION

We have shown that the topological and trivial phases are well differentiated in the mechanical rotator model even in a strong nonlinear regime based on the bulk-edge correspondence. Our finding is that the topological properties are inherited to the nonlinear model from the associated linearized model provided they are smoothly connected. Then, it would be possible to use a topological number defined in the linearized model. This phenomenon is quite similar to the one in the Toda lattice⁵⁶, which is a typical exactly solvable model containing a soliton.

The author is very much grateful to N. Nagaosa for helpful discussions on the subject. This work is supported by the Grants-in-Aid for Scientific Research from MEXT KAKENHI (Grants No. JP17K05490 and No. JP18H03676). This work is also supported by CREST, JST (JPMJCR16F1 and JPMJCR20T2).

¹ M. Z. Hasan and C. L. Kane, Rev. Mod. Phys. **82**, 3045 (2010).

² X.-L. Qi and S.-C. Zhang, Rev. Mod. Phys. **83**, 1057 (2011).

³ E. Prodan and C. Prodan, Phys. Rev. Lett. **103**, 248101 (2009).

⁴ Z. Yang, F. Gao, X. Shi, X. Lin, Z. Gao, Y. Chong and B. Zhang, Phys. Rev. Lett. **114**, 114301 (2015).

⁵ P. Wang, L. Lu and K. Bertoldi, Phys. Rev. Lett. **115**, 104302 (2015).

⁶ M. Xiao, G. Ma, Z. Yang, P. Sheng, Z. Q. Zhang and C. T. Chan,

Nat. Phys. **11**, 240 (2015).

⁷ C. He, X. Ni, H. Ge, X.-C. Sun, Y.-B. Chen, M.-H. Lu, X.-P. Liu, L. Feng and Y.-F. Chen, Nature Physics **12**, 1124 (2016).

⁸ H. Abbaszadeh, A. Souslov, J. Paulose, H. Schomerus and V. Vitelli, Phys. Rev. Lett. **119**, 195502 (2017).

⁹ H. Xue, Y. Yang, F. Gao, Y. Chong and B. Zhang, Nature Materials **18**, 108 (2019).

¹⁰ X. Ni, M. Weiner, A. Alu and A. B. Khanikaev, Nature Materials

- 18**, 113 (2019).
- ¹¹ M. Weiner, X. Ni, M. Li, A. Alu, A. B. Khanikaev, *Science Advances* **6**, eaay4166 (2020)
 - ¹² H. Xue, Y. Yang, G. Liu, F. Gao, Y. Chong and B. Zhang, *Phys. Rev. Lett.* **122**, 244301 (2019).
 - ¹³ C. L. Kane and T. C. Lubensky, *Nature Phys.* **10**, 39 (2014).
 - ¹⁴ B. Gin-ge Chen, N. Upadhyaya and V. Vitelli, *PNAS* **111**, 13004 (2014)
 - ¹⁵ L. M. Nash, D. Kleckner, A. Read, V. Vitelli, A. M. Turner and W. T. M. Irvine, *PNAS* **112**, 14495 (2015).
 - ¹⁶ J. Paulose, A. S. Meeussen and V. Vitelli, *PNAS* **112**, 7639 (2015)
 - ¹⁷ R. Susstrunk, S. D. Huber, *Science* **349**, 47 (2015).
 - ¹⁸ R. Susstrunk and S. D. Huber, *Proc. Natl. Acad. Sci. USA* **113**, E4767 (2016).
 - ¹⁹ S. D. Huber, *Nature Physics* **12**, 621 (2016).
 - ²⁰ A. S. Meeussen, J. Paulose and V. Vitelli, *Phys. Rev. X* **6**, 041029 (2016).
 - ²¹ T. Kariyado and Y. Hatsugai, *Sci. Rep.* **5**, 18107 (2016).
 - ²² T. Kariyado and Y. Hatsugai, *J. Phys. Soc. Jpn.* **85**, 043001 (2016).
 - ²³ H. C. Po, Y. Bahri and A. Vishwanath, *Phys. Rev. B* **93**, 205158 (2016).
 - ²⁴ D. Zeb Rocklin, Bryan Gin-ge Chen, Martin Falk, Vincenzo Vitelli, and T. C. Lubensky, *Phys. Rev. Lett.* **116**, 135503 (2016)
 - ²⁵ Y. Takahashi, T. Kariyado and Y. Hatsugai, *New J. Phys.* **19**, 035003 (2017).
 - ²⁶ K. H. Matlack, M. Serra-Garcia, A. Palermo, S. D. Huber and C. Daraio, *Nature Mat.* **17**, 323 (2018).
 - ²⁷ Y. Takahashi, T. Kariyado and Y. Hatsugai, *Phys. Rev. B* **99**, 024102 (2019).
 - ²⁸ A. Ghatak, M. Brandenbourger, J. van Wezel and C. Coulais, *Proc. Natl. Ac. Sc. U.S.A.* **117**, 29561 (2020)
 - ²⁹ H. Wakao, T. Yoshida, H. Araki, T. Mizoguchi and Y. Hatsugai, *Phys. Rev. B* **101**, 094107 (2020).
 - ³⁰ A. B. Khanikaev, S. H. Mousavi, W.-K. Tse, M. Kargarian, A. H. MacDonald, G. Shvets, *Nature Materials* **12**, 233 (2013).
 - ³¹ M. Hafezi, E. Demler, M. Lukin, J. Taylor, *Nature Physics* **7**, 907 (2011).
 - ³² M. Hafezi, S. Mittal, J. Fan, A. Migdall, J. Taylor, *Nature Photonics* **7**, 1001 (2013).
 - ³³ L.H. Wu and X. Hu, *Phys. Rev. Lett.* **114**, 223901 (2015).
 - ³⁴ L. Lu, J. D. Joannopoulos and M. Soljacic, *Nature Photonics* **8**, 821 (2014).
 - ³⁵ T. Ozawa, H. M. Price, A. Amo, N. Goldman, M. Hafezi, L. Lu, M. C. Rechtsman, D. Schuster, J. Simon, O. Zilberberg and L. Carusotto, *Rev. Mod. Phys.* **91**, 015006 (2019).
 - ³⁶ A. E. Hassan, F. K. Kunst, A. Moritz, G. Andler, E. J. Bergholtz, M. Bourennane, *Nature Photonics* **13**, 697 (2019)
 - ³⁷ M. Li, D. Zhirihin, D. Filonov, X. Ni, A. Slobozhanyuk, A. Alu and A. B. Khanikaev, *Nature Photonics* **14**, 89 (2020)
 - ³⁸ S. Imhof, C. Berger, F. Bayer, J. Brehm, L. Molenkamp, T. Kiessling, F. Schindler, C. H. Lee, M. Greiter, T. Neupert, R. Thomale, *Nat. Phys.* **14**, 925 (2018).
 - ³⁹ C. H. Lee, S. Imhof, C. Berger, F. Bayer, J. Brehm, L. W. Molenkamp, T. Kiessling and R. Thomale, *Communications Physics*, **1**, 39 (2018).
 - ⁴⁰ T. Helbig, T. Hofmann, C. H. Lee, R. Thomale, S. Imhof, L. W. Molenkamp and T. Kiessling, *Phys. Rev. B* **99**, 161114 (2019).
 - ⁴¹ Y. Lu, N. Jia, L. Su, C. Owens, G. Juzeliunas, D. I. Schuster and J. Simon, *Phys. Rev. B* **99**, 020302 (2019).
 - ⁴² Y. Li, Y. Sun, W. Zhu, Z. Guo, J. Jiang, T. Kariyado, H. Chen and X. Hu, *Nat. Com.* **9**, 4598 (2018)
 - ⁴³ M. Ezawa, *Phys. Rev. B* **98**, 201402(R) (2018).
 - ⁴⁴ K. Luo, R. Yu and H. Weng, *Research*, ID 6793752. (2018)
 - ⁴⁵ E. Zhao, *Ann. Phys.* **399**, 289 (2018).
 - ⁴⁶ M. Ezawa, *Phys. Rev. B* **99**, 201411(R) (2019).
 - ⁴⁷ M. Ezawa, *Phys. Rev. B* **99**, 121411(R) (2019).
 - ⁴⁸ M. Serra-Garcia, R. Susstrunk and S. D. Huber, *Phys. Rev. B* **99**, 020304 (2019).
 - ⁴⁹ T. Hofmann, T. Helbig, C. H. Lee, M. Greiter, R. Thomale, *Phys. Rev. Lett.* **122**, 247702 (2019).
 - ⁵⁰ M. Ezawa, *Phys. Rev. B* **100**, 045407 (2019).
 - ⁵¹ M. Ezawa, *Phys. Rev. B* **102**, 075424 (2020).
 - ⁵² C. H. Lee, T. Hofmann, T. Helbig, Y. Liu, X. Zhang, M. Greiter and R. Thomale, *Nature Communications* **11**, 4385 (2020).
 - ⁵³ T. Kotwal, H. Ronellenfitsch, F. Moseley, A. Stegmaier, R. Thomale, J. Dunkel, *PNAS* **118**, e2106411118 (2021)
 - ⁵⁴ D. Smirnova, D. Leykam, Y. Chong and Y. Kivshar, *Applied Physics Reviews* **7**, 021306 (2020)
 - ⁵⁵ K. Sone, Y. Ashida, T. Sagawa, *arXiv:2012.09479*
 - ⁵⁶ M. Ezawa, *cond-mat/arXiv:2105.10851*
 - ⁵⁷ M. Ezawa, *Phys. Rev. B* **100**, 165419 (2019).